

## Special Issue: V3-LAVA PROJECT

# RST<sub>VOLC</sub> implementation on MODIS data for monitoring of thermal volcanic activity

Teodosio Lacava<sup>1,\*</sup>, Francesco Marchese<sup>1</sup>, Nicola Pergola<sup>1</sup>, Valerio Tramutoli<sup>2,1</sup>, Irina Coviello<sup>1</sup>, Mariapia Faruolo<sup>1</sup>, Rossana Paciello<sup>1</sup>, Giuseppe Mazzeo<sup>1</sup>

<sup>1</sup> Istituto di Metodologie per l'Analisi Ambientale (IMAA), Consiglio Nazionale delle Ricerche, Tito Scalo (Potenza), Italy

<sup>2</sup> Università della Basilicata, Dipartimento di Ingegneria e Fisica dell'Ambiente (DIFA), Potenza, Italy

### Article history

Received November 22, 2010; accepted June 15, 2011.

### Subject classification:

Mount Etna, MODIS, hot spots, RST<sub>VOLC</sub>.

### ABSTRACT

An optimized configuration of the Robust Satellite Technique (RST) approach was developed within the framework of the 'LAVA' project. This project is funded by the Italian Department of Civil Protection and the Italian Istituto Nazionale di Geofisica e Vulcanologia, with the aim to improve the effectiveness of satellite monitoring of thermal volcanic activity. This improved RST configuration, named RST<sub>VOLC</sub>, has recently been implemented in an automatic processing chain that was developed to detect hot-spots in near real-time for Italian volcanoes. This study presents the results obtained for the Mount Etna eruption of July 14-24, 2006, using the Moderate Resolution Imaging Spectroradiometer (MODIS) data. To better assess the operational performance, the RST<sub>VOLC</sub> results are also discussed in comparison with those obtained by MODVOLC, a well-established, MODIS-based algorithm for hot-spot detection that is used worldwide.

### 1. Introduction

The Robust Satellite Technique (RST) approach [Tramutoli 2007] is a multi-temporal scheme of satellite data analysis that was proposed to study and monitor active volcanoes [Pergola et al. 2004]. An enhanced RST-based algorithm, named RST<sub>VOLC</sub> [Marchese et al. 2011], was developed to further improve the performance for volcanic hot-spot detection. RST<sub>VOLC</sub> has been tested operationally in the framework of the recent 'LAVA' project, which is funded by the Italian Department of Civil Protection and the Istituto Nazionale di Geofisica e Vulcanologia [INGV 2010]. RST<sub>VOLC</sub> offers the same advantages as RST (e.g. independence from site/ seasonal effects, like high reflectance of sparsely vegetated areas, emissivity variations, and natural warming of volcanic rock) [Di Bello et al. 2004, Pergola et al. 2004]. It guarantees an improved trade-off between reliability and sensitivity, which makes it more suitable for operational monitoring of active volcanoes [Marchese et al. 2011].

Within the LAVA project, RST<sub>VOLC</sub> was implemented on

data from the Advanced Very-High-Resolution Radiometer (AVHRR) of the National Oceanic and Atmospheric Administration (NOAA), and for the first time, on data from the Moderate-Resolution Imaging Spectroradiometer (MODIS) of the Earth Observing Systems (EOS). These data were directly acquired from the laboratories of the Institute of Methodologies for Environmental Analysis (IMAA, Potenza, Italy) and the Department of Engineering and Physics of the Environment (DIFA, Potenza, Italy).

The RST<sub>VOLC</sub> implementation on the MODIS data allowed us to exploit the better spectral features of this sensor in comparison with the AVHRR. Indeed, MODIS offers two middle infrared (MIR) channels (bands 21 and 22) in the range of 3.92  $\mu\text{m}$  to 3.98  $\mu\text{m}$ , with a radiometric accuracy of 2.0 K and 0.07 K, respectively. In addition, band 22 saturates at a brightness temperature of 330 K, while although characterized by lower data quality, band 21 offers a higher saturation level up to 500 K. This makes band 21 particularly suitable for the identification of high-temperature surfaces (e.g. lava bodies).

A full integration of multi-sensor data (i.e. AVHRR + MODIS) guarantees an increased frequency of observation, which is required especially when rapidly evolving phenomena have to be investigated, such as volcanic eruptions. The Mount Etna eruption that occurred from July 14-24, 2006, was analyzed to test the RST<sub>VOLC</sub> performance for the monitoring of thermal volcanic activity. This eruption was chosen in particular as the case study because it was short in time (i.e. it lasted for only 10 days) and it was sufficiently documented by volcanological reports (INGV-CT, 2006; Smithsonian Institution, 2006). As RST<sub>VOLC</sub> is here applied for the first time to these MODIS data, to better assess its performance, the results obtained have also been compared with those from MODVOLC [Wright et al. 2002, 2004], a well-established and widely used MODIS-based method for automated volcanic hot-spot detection and

monitoring that represents a benchmark in this field [e.g. Hirn et al. 2009, Delle Donne et al. 2010, Lyons et al. 2010].

## 2. Test case: the Mount Etna eruption of July 14-24, 2006

On July 14, 2006, at around 23:30 local time (21:30 GMT), an eruptive fissure opened on the east flank of the South East Crater of Mount Etna (Figure 1). Two vents located along the fissure emitted lava flows that spread 3 km East to the Valle del Bove [Smithsonian Institution 2006]. A moderate strombolian eruption also occurred at another vent, on the Eastern flank of the South East Crater, which produced ash fallout on the city of Catania [INGV-CT 2006]. On July 17, 2006, two main lava-flow fronts reached an altitude of about 2,100 m above sea level, spreading North of the Serra Giannicola Piccola ridge. On July 18, 2006, there was a further explosive activity similar to that on the day before, with emission of high-temperature gases [INGV-CT 2006, Smithsonian Institution 2006]. At an altitude of about 2,275 m, the lava flows spread into two main branches. On July 19, 2006, a new explosive vent opened that emitted ash and pyroclastic products. After the ash emissions, there was an increase in the effusion rate [INGV-CT 2006, Smithsonian Institution 2006] and some strong strombolian eruptions. On July 20, 2006, the lava discharge reached its peak, with an effusion rate of between 10 m<sup>3</sup>/s and 14 m<sup>3</sup>/s [Héroult et al. 2009], and intense and continuous strombolian activity also occurred at the volcano [Smithsonian Institution 2006]. On July 21, 2006, there was an increase in the explosive activity, while on July 22, 2006, the lava reached Mount Centenari, at an altitude of 1,750 m. Another lava body was also emitted from an effusive vent at an altitude of about 2,800 m. On July 23, 2006, the new lava effusion stopped, and there were

reduced effusion rates from the main vents. No explosive activity was observed at the eruptive cone. On July 24, 2006, a helicopter survey reported a reduction in the activity of the eruptive vents, and the end of the effusive eruption was declared [INGV-CT 2006, Smithsonian Institution 2006].

## 3. RST<sub>VOLC</sub> implementation on the MODIS data

A detailed description of the RST<sub>VOLC</sub> technique can be found in Marchese et al. [2011]. Briefly, RST<sub>VOLC</sub> combines two local variation indices,  $\otimes_{\text{MIR}}(x,y,t)$  and  $\otimes_{\text{MIR-TIR}}(x,y,t)$ , to automatically detect volcanic hot-spots, as defined as:

$$\otimes_{\text{MIR}}(x,y,t) = \frac{[T_{\text{MIR}}(x,y,t) - \mu_{\text{MIR}}(x,y)]}{\sigma_{\text{MIR}}(x,y)} \quad (1)$$

$$\otimes_{\text{MIR-TIR}}(x,y,t) = \frac{[\Delta T(x,y,t) - \mu_{\Delta T}(x,y)]}{\sigma_{\Delta T}(x,y)} \quad (2)$$

In Equation (1),  $T_{\text{MIR}}(x,y,t)$  is the satellite signal (in terms of the brightness temperature) measured in the MIR spectral band between 3 μm and 4 μm, which is the most suitable for the identification of high-temperature surfaces [e.g. Harris et al. 1995], at place  $(x,y)$  and time  $t$ .  $\mu_{\text{MIR}}(x,y)$  and  $\sigma_{\text{MIR}}(x,y)$  are the temporal mean and temporal standard deviation (i.e. the spectral reference fields) of these signals, respectively, which are derived from long time series of homogeneous (e.g. same calendar month and same hour of pass) cloud-free satellite records.

In Equation (2),  $\Delta T = T_{\text{MIR}} - T_{\text{TIR}}$  is the difference in the brightness temperatures measured in the MIR and Thermal Infrared (TIR) spectral bands, while  $\mu_{\Delta T}$  and  $\sigma_{\Delta T}$  have the same meaning as above.

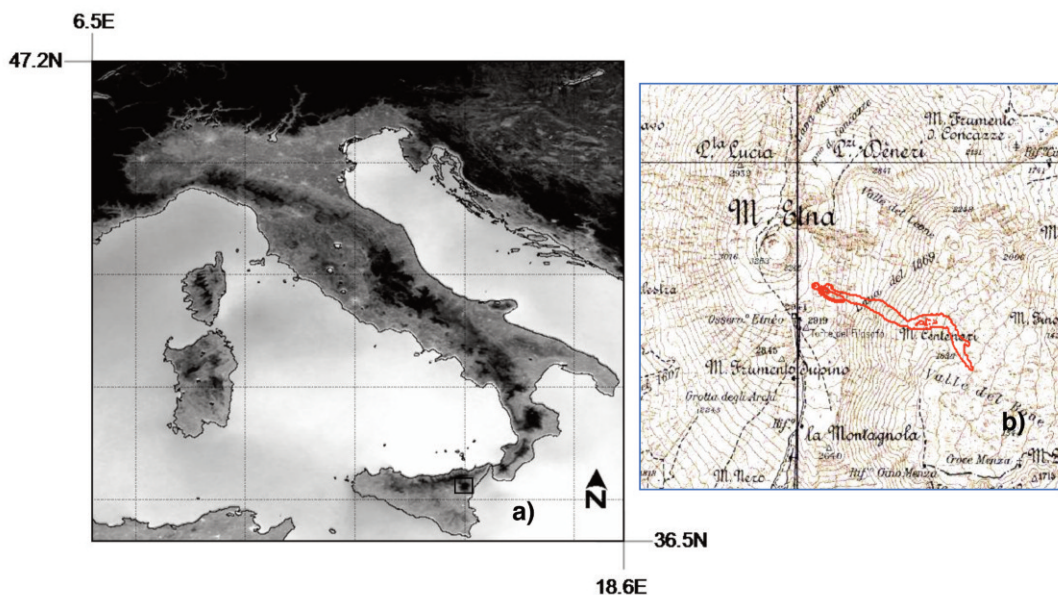


**Figure 1.** a) The sub-scene extracted from the original Level 1b MODIS data reprojected in LAT/LONG WGS84 that was used by RST<sub>VOLC</sub> for data processing, showing the Mount Etna area (blue square). b) Map of the lava flow at Mount Etna of July 24, 2006 (from the Italian Department of Civil Protection – Istituto Nazionale di Geofisica e Vulcanologia V3 LAVA project [INGV 2010]).

The  $\otimes_{\text{MIR-TIR}}(x,y,t)$  index is applied after the  $\otimes_{\text{MIR}}(x,y,t)$  index, which is more protected by local and atmospheric effects [Pergola et al. 2004]. This serves to remove residual spurious effects that are related to natural signal fluctuations (i.e. anomalous increases in the surface temperature because of weather/climatic conditions). On the one hand, high values of both of these local variation indices are expected in the presence of ‘actual’ volcanic hot-spots. On the other hand, low values of the  $\otimes_{\text{MIR-TIR}}(x,y,t)$  index should characterize spurious effects related to natural signal fluctuations that show similar behaviors in the MIR and TIR spectral bands [Marchese et al. 2011]. According to the aims of the present study, 1,237 MODIS images were acquired and processed for channels 22 (or 21 when the previous one was saturated) (MIR) and 31 (TIR) during the months of July of 2000 to 2009 (i.e. July 2000, July 2001..., July 2009). The selected imagery were separated into two different datasets: one including diurnal data (605 images) and the other including only nocturnal overpasses (632 images) from both the EOS-Terra and EOS-Aqua satellites. The two datasets were populated by the selection of the data acquired from 09.30 to 13.30 GMT (LT=GMT+2) and from 21.30 to 01.30 GMT, respectively. A RST-based cloud detection scheme, named as the One-Channel Cloudy Radiance Detection Approach (OCA) [Pietrapertosa et al. 2001, Cuomo et al. 2004], was then applied to remove the cloudy pixels from the scenes before the computation of the spectral reference fields. The satellite images were processed and precisely co-located in the space-time domain, with the extraction for each overpass of a sub-scene of size  $1211 \times 1070$  (see Figure 1), which was centered over the Mediterranean basin, and was reprojected in Lat-Long (WGS84) projection using the nearest-neighbor resampling method.

#### 4. Results and discussion

The  $\otimes_{\text{MIR}}(x,y,t)$  and  $\otimes_{\text{MIR-TIR}}(x,y,t)$  indices are defined as two standardized variables that have a Gaussian behavior. As an example, Figure 2 shows the statistical behavior of the  $\otimes_{\text{MIR}}(x,y,t)$  index computed for a single unperturbed pixel close to the volcanic edifice, from an analysis of 10 years of satellite records. The index behavior is well fitted by a Gaussian curve ( $R^2 = 0.96$ ), with mean value  $\mu = 0.13$  and standard deviation  $\sigma = 1.1$ . In this case, the slight asymmetry of the histogram towards negative values is due to residual-cloud contamination effects. Considering that for a normal distribution, about 99.7% of the data ( $x$ ) is included in the range ‘ $\mu - 3\sigma < x < \mu + 3\sigma$ ’, values of  $\otimes_{\text{MIR}}(x,y,t) > 3$  should occur with a probability around 0.15%, and they thus represent statistically significant anomalies. Similarly, the same behavior can be addressed to the  $\otimes_{\text{MIR-TIR}}(x,y,t)$  index. Therefore, the values of ‘ $\otimes_{\text{MIR}}(x,y,t) > 3$  AND  $\otimes_{\text{MIR-TIR}}(x,y,t) > 3$ ’ are generally used by RST<sub>VOLC</sub> to identify volcanic hot-spots. In this case, because of the multiplication rule, the

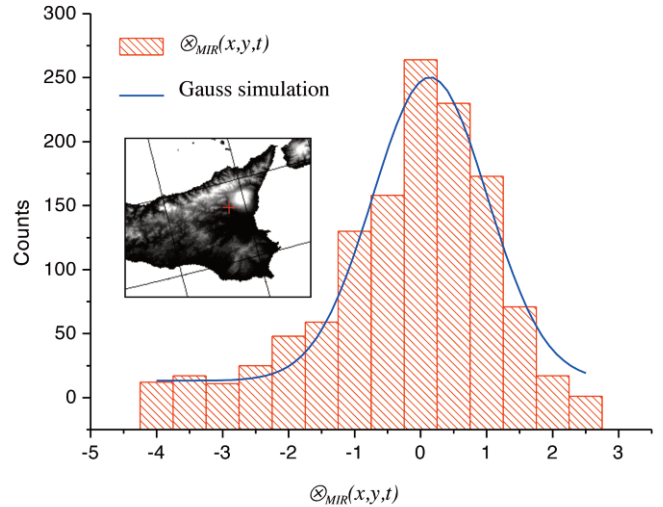


**Figure 2.** Histogram of the  $\otimes_{\text{MIR}}(x,y,t)$  index computed for a single unperturbed pixel selected over a nonvolcanic area close to the Mount Etna edifice on ten years of satellite records, with mean =  $-0.13$  and sigma =  $1.13$ . Inset: Digital elevation model GTOPO 100 with red cross to indicate the location of the unperturbed pixel.

probability of occurrence is even lower (0.0225%), and consequently, the anomalies detected should be even more significant from a statistical point of view.

The hot-spots detected by RST<sub>VOLC</sub> from the processing of 42 MODIS overpasses acquired from July 15-24, 2006, are reported in Table 1. They are in good agreement with the available field observations of the Mount Etna activity over this investigated time period [e.g. INGV-CT 2006, Smithsonian Institution 2006].

Starting from the first MODIS image that was available after the onset of the eruption, namely that acquired on July 15, 2006, at 01:35 GMT (about four hours after the onset), volcanic hot-spots were detected by RST<sub>VOLC</sub> with a good level of continuity, apart from some cloudy scenes where the target area was completely masked by weather clouds (see Table 1). Figure 3 reports the number of hot-spots detected each day during the eruptive period investigated, which gives an indication of the space-time evolution of the thermal phenomena that was in progress at Mount Etna. In particular, the time series shows the occurrence of two distinct eruptive phases for the volcano: the first was characterized by a continuous and marked increase in the daily number of hot-spots from the beginning of the eruptive activity until its paroxysmal phase; the second was characterized by a decrease in the daily number of hot-spots after July 22, 2006, until the end of the eruption.

The slight decrease in the number of thermal anomalies detected on July 17 and 19, 2006, is related to the high satellite zenith angles of most of the MODIS satellite overpasses that were acquired for these days (e.g. on July 17, 2006, all of passes had satellite zenith angles  $\geq 40^\circ$ ). At such view angles, a reduction in the sensor-measured radiance has

Date [YY/MM/DD hhmmss]	Satellite	Hot-spots detected by $RST_{VOLC}$	Satellite zenith angle ( $^{\circ}$ )
06/07/15 013500	Aqua	2	56
06/07/15 092500	Terra	0 (cloudy)	43
06/07/15 124000	Aqua	0 (cloudy)	53
06/07/15 203000	Terra	5	48
06/07/16 004000	Aqua	5	25
06/07/16 100500	Terra	0 (cloudy)	29
06/07/16 114500	Aqua	5	33
06/07/16 211500	Terra	5	21
06/07/17 012500	Aqua	4	45
06/07/17 091000	Terra	1	55
06/07/17 123000	Aqua	2	40
06/07/17 202000	Terra	5	58
06/07/18 003000	Aqua	8	43
06/07/18 095500	Terra	3	8
06/07/18 113500	Aqua	0 (cloudy)	48
06/07/18 210000	Terra	7	1
06/07/19 011000	Aqua	6	29
06/07/19 090000	Terra	2	64
06/07/19 104000	Terra	2	60
06/07/19 122000	Aqua	4	21
06/07/19 214500	Terra	2	58
06/07/20 001500	Aqua	7	55
06/07/20 094500	Terra	4	15
06/07/20 112500	Aqua	3	58
06/07/20 205000	Terra	11	25
06/07/21 010000	Aqua	10	8
06/07/21 102500	Terra	2	51
06/07/21 120500	Aqua	5	1
06/07/21 213000	Terra	6	47
06/07/22 000500	Aqua	6	64
06/07/22 014500	Aqua	2	60
06/07/22 093000	Terra	6	35
06/07/22 125000	Aqua	1	58
06/07/22 203500	Terra	9	41
06/07/23 004500	Aqua	8	15
06/07/23 101500	Terra	2	38
06/07/23 115500	Aqua	3	23
06/07/23 212000	Terra	3	31
06/07/24 013000	Aqua	2	51
06/07/24 092000	Terra	0 (cloudy)	50
06/07/24 123500	Aqua	0 (cloudy)	47
06/07/24 202500	Terra	1	53

**Table 1.** Hot-spots detected by  $RST_{VOLC}$  over the Mount Etna area from July 15–24, 2006, with dates of detection, the satellites for the sensing, and the relative satellite zenith angles.

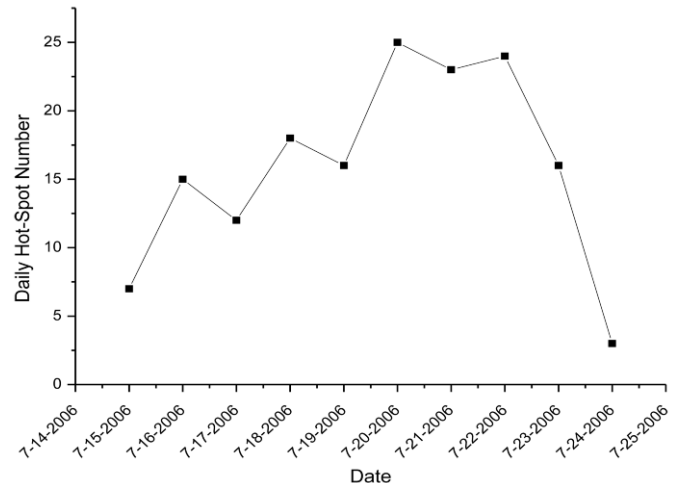


**Figure 3.** Time series of the number of daily hot-spots detected by  $RST_{VOLC}$  through the analysis of all of the MODIS data acquired over the target area (Mount Etna) for the period of July 15–24, 2006.

to be expected [Coppola et al. 2010], even if the relative impact of this effect also depends on the intensity (e.g. temperature and extent) of the thermal source.

Major peaks in the daily number of hot-spots were recorded between July 20 and 22, 2006, in good agreement with the observed increase in lava effusion [Héroult et al. 2009]. The strong drop in the daily number of hot-spots on July 23, 2006, was instead in agreement with a significant reduction in the eruption intensity that was reported by volcanological bulletins on that day [INGV-CT 2006, Smithsonian Institution 2006].

These results confirm the potential of  $RST_{VOLC}$  for the monitoring of thermal volcanic activity. They also integrate and complete our previous studies on the same eruptive event, which were performed using both the AVHRR and SEVIRI data [Pergola et al. 2008], confirming the independence of this RST approach on satellite platforms.

In addition, to better assess the  $RST_{VOLC}$  results (here applied for the first time to MODIS imagery), a comparison with the MODVOLC results was also carried out. MODVOLC is one of the most well-established MODIS-based methods for satellite hot-spot detection, and it has been implemented in an automatic system that was developed for near real-time monitoring of volcanoes at a global scale [Wright et al. 2002]. The MODVOLC products are continuously posted on the internet, about 20 h after the sensing time [MODVOLC 2002–2010]. This method computes a normalized thermal index (NTI) to detect the volcanic hot-spots, which are calculated on the basis of the MIR and TIR radiances measured in the MODIS channels 21 or 22, and 32, respectively. For the nighttime data, the image pixels with a NTI index greater than ‘-0.80’ are flagged as hot-spots [Wright et al. 2002, 2004]. Instead, to take into account the solar reflected component of the MIR radiance in the daytime, a correction for the reflected

solar radiation is performed using the MODIS short-wave infrared band centered at 1.6  $\mu\text{m}$  (i.e. channel 6) (<http://modis.higp.hawaii.edu/daytime.html>). Once this correction is performed, the hot-spots are identified by MODVOLC when the NTI index exceeds '-0.60'.

MODVOLC was designed to work under some specific restrictions that were imposed by the computer resources available in 2000 at the Distributed Active Archive Center of the Goddard Space Flight Center. Among these restrictions, one is related to the use of Level 1b MODIS data.

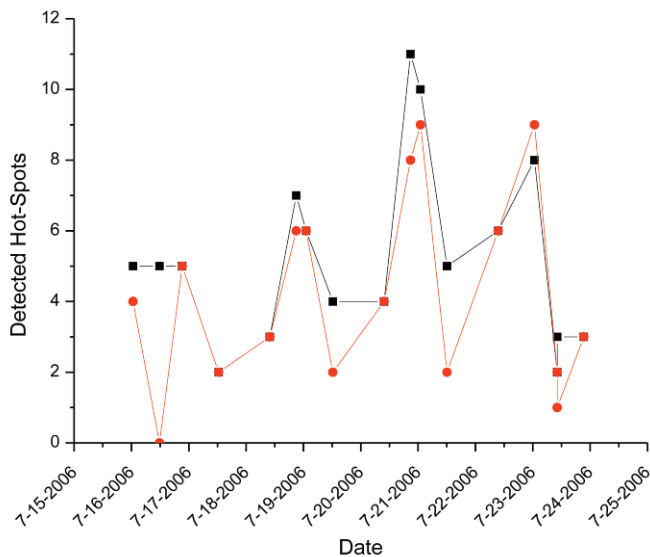


**Figure 4.** Hot-spots detected by RST<sub>VOLC</sub> (black) and by MODVOLC (red), for the Mount Etna eruption of July 15–24, 2006, from the processing of the MODIS data acquired with satellite zenith angles  $<40^\circ$  (see main text).

Unfortunately, at high satellite zenith angles, these Level 1b MODIS data are affected by bow-tie [Landesa et al. 2004]. It is an artefact of the images related to the arrangement of the detectors that can duplicate detected hot-spots due to oversampling at the borders of the scene [Coppola et al. 2010]. Therefore, to avoid bow-tie-related artefacts, in the present study, the RST<sub>VOLC</sub> products were compared to those of MODVOLC, considering only the data acquired at low satellite zenith angles (i.e.  $<40^\circ$ ). As independently demonstrated by other studies, these should be less affected by such effects [e.g. Coppola et al. 2010]. Figure 4 shows the number of hot-spots detected by RST<sub>VOLC</sub> and MODVOLC, for all the MODIS overpasses acquired under these specific conditions. There is a good agreement between the two hot-spot curves (Figure 4). Both of these curves appear to correctly describe the time evolution of the eruptive event, with major peaks in the number of hot-spots detected between July 20 and 21, 2006, and with a significant intensity decrease starting from July 23, 2006.

However, despite this agreement, some differences can also be noted. The most significant difference in the number of hot-spots is evident on seen for the MODIS overpass of July 16, 2006, at 11:45 UTC. In this case, although five hot-spots were correctly detected by RST<sub>VOLC</sub> over the Mount Etna area, no hot-spot was identified by MODVOLC. This difference, which is not evaluable by just examining of the MODVOLC products that are available online, required the MODVOLC implementation on MODIS Level 1b data to be fully interpreted.

On the basis of this data investigation, it was evident that no hot-spot was identified by MODVOLC over the

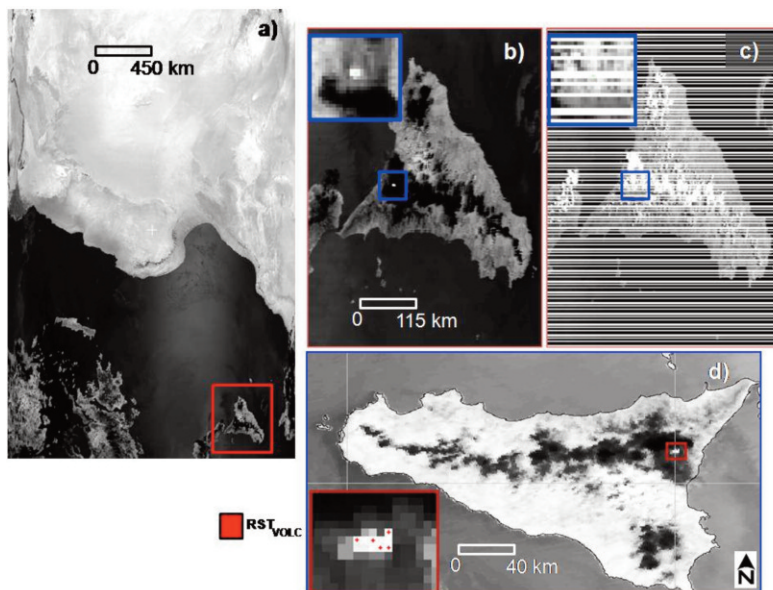


**Figure 5.** a) Level 1b MODIS channel 22 image of July 16, 2006, at 11:45 GMT (13:45 LT). b) Enlargement of the area within the red box in (a). c) Level 1b MODIS channel 6 image of the same MODIS overpass, with evidence of striping effects on the MODVOLC detection. d) Original MODIS image with red crosses to indicate the locations of the pixels corresponding to the hot-spots detected by RST<sub>VOLC</sub>.

Mount Etna area because of the striping effects that affect AQUA-MODIS band 6. Indeed, Figure 5a,b shows the actual hot-spots related to an eruptive activity in progress on Mount Etna that were not identified by MODVOLC, because located over some striping lines of the MODIS band 6 (see Figure 5c). These hot spots were correctly detected, instead, by RST<sub>VOLC</sub> (Figure 5d). Striping problems related to 15 noisy AQUA detectors [Salomonson and Appel 2006, NASA GSFC 2010] affected each daytime AQUA-MODIS overpass that was analyzed in this study (10 in total), which accounted for the main cause of differences in the hot-spot numbers detected by RST<sub>VOLC</sub> and by MODVOLC.

It should be noted that these striping effects, like bow-tie, cannot be directly ascribed to the MODVOLC algorithm, as they are instead issues of MODIS Level 1b data. Moreover, in principle, these effects can be removed by implementation of a pre-processing, de-striping procedure that when applied before the NTI index computation, might improve the daytime MODVOLC performance. Instead, for the slight differences in the hot-spot numbers of Figure 4 that were observed mainly in the night-time records, these were related to the known reduction in sensitivity of MODVOLC in the presence of subtle hot-spots [Wright et al. 2002, 2004, Kervyn et al. 2006, 2008]. This is a consequence of the fixed detection thresholds used by MODVOLC to monitor volcanoes at a global scale.

As further confirmation of this issue, the authors of MODVOLC have recently proposed a hybrid approach that combines MODVOLC with a RST-based time series [Koeppen et al. 2010]. The results that arise from the comparison with MODVOLC confirm the performances of RST<sub>VOLC</sub> for the successful monitoring of thermal volcanic activity using the MODIS data. It should be stressed that by using local adaptive thresholds that are specific for each place and time of observation, the RST<sub>VOLC</sub> technique can be used to effectively monitor volcanoes at different geographic locations, requiring only a historical dataset of satellite records to be applied.

## 5. Conclusions

In the present study, the outcomes of the Italian Department of Civil Protection – Istituto Nazionale di Geofisica e Vulcanologia ‘LAVA’ project that were obtained for the development and testing of the RST<sub>VOLC</sub> technique have been presented and discussed. These results highlight the performance of the RST<sub>VOLC</sub> for the detection of volcanic hot-spots under different observational conditions by using the MODIS data. As these data are based only on satellite records, RST<sub>VOLC</sub> can be exported easily on whatever kind of satellite/sensor system, provided that multi-year time series imagery is available. In addition, the successful real-time experimentation of hot-spot products that was performed in the framework of the LAVA project has confirmed the potential of RST<sub>VOLC</sub> in the monitoring of volcanoes under

possible operational scenarios. Finally, the comparison of the RST<sub>VOLC</sub> and MODVOLC results has shown similar capabilities of these two methods for the monitoring of the thermal activity that was in progress on Mount Etna during July 2006. This analysis also indicates that MODVOLC might benefit from a pre-processing procedure that includes data de-striping, which, if applied before the NTI index, might improve its performance under daytime conditions.

**Acknowledgements.** This study received financial support from the V3-LAVA project (Italian Department of Civil Protection – Istituto Nazionale di Geofisica e Vulcanologia, 2007-2009 contract).

## References

- Coppola, D., M.R. James, T. Staudacher and C. Cigolini (2010). A comparison of field- and satellite-derived thermal flux at Piton de la Fournaise: implications for the calculation of lava discharge rate, *B. Volcanol.*, 72, 341-356; doi: 10.1007/s00445-009-0320-8.
- Cuomo, V., C. Filizzola, N. Pergola, C. Pietrapertosa and V. Tramutoli (2004). A self sufficient approach for Gerb cloudy radiance detection, *Atmos. Res.*, 72, 39-56.
- Delle Donne, D., A.J.L. Harris, M. Ripepe and R. Wright (2010). Earthquake-induced thermal anomalies at active volcanoes, *Geology*, 38, 771-774.
- Di Bello, G., C. Filizzola, T. Lacava, F. Marchese, N. Pergola, C. Pietrapertosa , S. Piscitelli, I. Scaffidi and V. Tramutoli (2004). Robust satellite techniques for volcanic and seismic hazards monitoring, *Annals of Geophysics*, 47 (1), 49-64.
- Harris, A.J., S.E.J. Swabey and J. Higgins (1995). Automated threshold 463 of active lava using AVHRR data, *Int. J. Remote Sens.*, 16, 3681-3686.
- Héault, A., A. Vicari, A. Cirauco and C. Del Negro (2009). Forecasting lava flow hazards during the 2006 Etna eruption: Using the MAGFLOW cellular automata model, *Comput. Geosci.-UK*, 35 (5), 1050-1060; doi: 10.1016/j.cageo.2007.10.008.
- Hirn, B., C. Di Bartola and F. Ferrucci (2009). Combined Use of SEVIRI and MODIS for Detecting, Measuring, and Monitoring Active Lava Flows at Erupting Volcanoes, *IEEE T. Geosci. Remote*, 47, 2923-2930.
- INGV-CT (2006). Reports on volcanic activity-U.F. Vulcanologia e Geochimica. Available from Istituto Nazionale di Geofisica e Vulcanologia, Sezione di Catania, Italy.
- INGV (2010). Progetto V3 LAVA. Realizzazione della mappa di pericolosità da colate di lava all'Etna, e messa a punto di un metodo di aggiornamento dinamico. Available at: [http://istituto.ingv.it/l-ingv/progetti/progetti-finanziati-dal-dipartimento-di-protezione-civile-1/progetti-dpc-convenzione-2007-2009/progetti\\_v/V3/V3-Lava](http://istituto.ingv.it/l-ingv/progetti/progetti-finanziati-dal-dipartimento-di-protezione-civile-1/progetti-dpc-convenzione-2007-2009/progetti_v/V3/V3-Lava) (in Italian).
- Lyons, J.J., G.P. Waite, W.I. Rose and G. Chigna (2010). Pat-

- terns in open vent, strombolian behavior at Fuego volcano, Guatemala, 2005-2007, *B. Volcanol.*, 72, 1-15.
- Kervyn, M., A. Harris, E. Mbede, F. Belton, P. Jacobs and G. G.J. Ernst (2006). MODLEN: A semi-automated algorithm for monitoring small-scale thermal activity at Oldoinyo Lengai volcano, Tanzania, In: Quantitative Geology from Multiple Sources, Proceedings of the XIth IAMG Annual Conference (Liège, Belgium, 3-8 September 2006).
- Kervyn, M., G.G. J. Ernst, A. Harris, E. Mbede, F. Belton and P. Jacobs (2008). Thermal remote sensing of the low-intensity carbonatite volcanism of Oldoinyo Lengai, Tanzania, *Int. J. Remote Sens.*, 29, 6467-6499.
- Koeppen, W.C., E. Pilger and R. Wright (2010). Time series analysis of infrared satellite data for detecting thermal anomalies: a hybrid approach, *B. Volcanol.*; doi: 10.1007/s00445-010-0427-y.
- Landesa, E.G., A. Rango and M. Bleiweiss (2004). An algorithm to address the MODIS bow-tie effects, *Can. J. Remote Sens.*, 30, 644-650.
- Marchese, F., C. Filizzola, N. Genzano, G. Mazzeo, N. Pergola and V. Tramutoli (2011). Assessment and improvement of a robust satellite technique (RST) for thermal monitoring of volcanoes, *Remote Sens. Environ.*, 115, 1556-1563; doi: 10.1016/j.rse.2011.02.014.
- MODVOLC (2002-2010). Near real-time thermal monitoring of global hot-spots, available at: <http://modis.higp.hawaii.edu/cgi-bin/modis/modisnew.cgi>.
- NASA GSFC (2010). MODIS history and performance: time-dependent list of non-functional or noisy detector, available at: <http://mcst.gsfc.nasa.gov/index.php?section=78>.
- Pergola, N., F. Marchese and V. Tramutoli (2004). Automated detection of thermal features of active volcanoes by means of infrared AVHRR records, *Remote Sens. Environ.*, 93, 311-327.
- Pergola, N., F. Marchese, V. Tramutoli, C. Filizzola and M. Ciampa (2008). Advanced satellite technique for volcanic activity monitoring and early warning, *Annals of Geophysics*, 51 (1), 287-301.
- Pietrapertosa, C., N. Pergola, V. Lanorte and V. Tramutoli (2001). Self adaptive algorithms for change detection: OCA (the One-channel Cloud-detection Approach) an adjustable method for cloudy and clear radiances detection, In: J.F. Le Marshall and J.D. Jasper (eds.), Technical Proceedings of the 11th International (A)TOVS Study Conference (ITSC-XI; Budapest, Hungary, 20-26 September 2000), published by Bureau of Meteorology Research Centre, Melbourne, Australia, 281-291.
- Smithsonian Institution (2006). Bulletin of the Global Volcanism Network, [http://www.volcano.si.edu/world/volcano.cfm?vnum=0101-06=&volpage=var#bgvn\\_3107](http://www.volcano.si.edu/world/volcano.cfm?vnum=0101-06=&volpage=var#bgvn_3107), 2006.
- Salomonson, V.V. and I. Appel (2006). Development of the aqua MODIS NDSI fractional snow cover algorithm and validation results, *IEEE T. Geosci. Remote*, 44, 1747-1756.
- Tramutoli, V. (2007). Robust Satellite Techniques (RST) for Natural and Environmental Hazards Monitoring and Mitigation: Theory and Applications, Proceedings of Multitemp 2007; doi: 10.1109/MULTITEMP.2007.4293057.
- Wright, R., L. Flynn, H. Garbeil, A. Harris and E. Pilger (2002). Automated volcanic eruption detection using MODIS, *Remote Sens. Environ.*, 82, 135-155.
- Wright, R., L.P. Flynn, H. Garbeil, A.J.L. Harris and E. Pilger (2004). MODVOLC: near-real-time thermal monitoring of global volcanism, *J. Volcanol. Geoth. Res.*, 135, 29-49.

---

\*Corresponding author: Teodosio Lacava,  
Istituto di Metodologie per l'Analisi Ambientale (IMAA),  
Consiglio Nazionale delle Ricerche, Tito Scalo (Potenza), Italy;  
email: lacava@imaa.cnr.it.